Singlet Benchmarks for LHC Run II

Tania Robens[1,*] and Tim Stefaniak[2,†]

[1] *TU Dresden, Institut für Kern- und Teilchenphysik, Zellescher Weg 19, D-01069 Dresden, Germany*

[2] *Department of Physics and Santa Cruz Institute for Particle Physics, University of California, Santa Cruz, CA 95064, USA*

(Dated: August 31, 2015)

Abstract

Benchmark points and planes for the real singlet extension of the SM Higgs sector for the LHC run II. Largely based on [1], with additional input from [2, 3].

*Electronic address: Tania.Robens@tu-dresden.de

†Electronic address: tistefan@ucsc.edu

Contents

I. THE MODEL

We here only list the features which are important in terms of benchmark choices and refer the the literature (cf. e.g. [1]) for more details.

A. Potential and couplings

The real Higgs singlet extension of the SM [4–6] contains a complex $SU(2)_L$ doublet, in the following denoted by Φ, and in additional a real scalar S which is a singlet under all SM gauge groups. The most generic renormalizable Lagrangian is then given by

$$\mathscr{L}_s = (D^\mu \Phi)^\dagger D_\mu \Phi + \partial^\mu S \partial_\mu S - V(\Phi, S)\,, \tag{1}$$

with the scalar potential

$$\begin{aligned} V(\Phi, S) &= -m^2 \Phi^\dagger \Phi - \mu^2 S^2 + \begin{pmatrix} \Phi^\dagger \Phi & S^2 \end{pmatrix} \begin{pmatrix} \lambda_1 & \frac{\lambda_3}{2} \\ \frac{\lambda_3}{2} & \lambda_2 \end{pmatrix} \begin{pmatrix} \Phi^\dagger \Phi \\ S^2 \end{pmatrix} \\ &= -m^2 \Phi^\dagger \Phi - \mu^2 S^2 + \lambda_1 (\Phi^\dagger \Phi)^2 + \lambda_2 S^4 + \lambda_3 \Phi^\dagger \Phi S^2. \end{aligned} \tag{2}$$

Here, we implicitly impose a Z_2 symmetry which forbids all linear or cubic terms of the singlet field S in the potential. We assume that both Higgs fields Φ and S have a non-zero vacuum expectation value (VEV), denoted by v and x, respectively. In the unitary gauge, the Higgs fields are given by

$$\Phi \equiv \begin{pmatrix} 0 \\ \frac{\tilde{h} + v}{\sqrt{2}} \end{pmatrix}, \qquad S \equiv \frac{h' + x}{\sqrt{2}}. \tag{3}$$

This leads to eigenstates with mass eigenvalues

$$m_h^2 = \lambda_1 v^2 + \lambda_2 x^2 - \sqrt{(\lambda_1 v^2 - \lambda_2 x^2)^2 + (\lambda_3 x v)^2}, \tag{4}$$

$$m_H^2 = \lambda_1 v^2 + \lambda_2 x^2 + \sqrt{(\lambda_1 v^2 - \lambda_2 x^2)^2 + (\lambda_3 x v)^2}, \tag{5}$$

where h and H are the scalar fields with masses m_h and m_H respectively, and $m_h^2 \leq m_H^2$ by convention. The gauge and mass eigenstates are related via the mixing matrix

$$\begin{pmatrix} h \\ H \end{pmatrix} = \begin{pmatrix} \cos\alpha & -\sin\alpha \\ \sin\alpha & \cos\alpha \end{pmatrix} \begin{pmatrix} \tilde{h} \\ h' \end{pmatrix}, \tag{6}$$

where the mixing angle $-\frac{\pi}{2} \leq \alpha \leq \frac{\pi}{2}$ is given by

$$\sin 2\alpha = \frac{\lambda_3 x v}{\sqrt{(\lambda_1 v^2 - \lambda_2 x^2)^2 + (\lambda_3 x v)^2}}, \tag{7}$$

$$\cos 2\alpha = \frac{\lambda_2 x^2 - \lambda_1 v^2}{\sqrt{(\lambda_1 v^2 - \lambda_2 x^2)^2 + (\lambda_3 x v)^2}}. \tag{8}$$

It follows from Eq. (6) that the light (heavy) Higgs boson couplings to SM particles are suppressed by $\cos\alpha\,(\sin\alpha)$.

If kinematically allowed, the additional decay channel $H \to hh$ is present. Its partial decay width is given by [4, 6]

$$\Gamma_{H\to hh} \;=\; \frac{|\mu'|^2}{8\pi m_H}\sqrt{1-\frac{4m_h^2}{m_H^2}}\,, \tag{9}$$

where the coupling strength μ' of the $H \to hh$ decay reads

$$\mu' = -\frac{\sin(2\alpha)}{2vx}\,(\sin\alpha v + \cos\alpha\, x)\left(m_h^2 + \frac{m_H^2}{2}\right). \tag{10}$$

We therefore obtain as branching ratios for the *heavy* Higgs mass eigenstate m_H

$$\begin{aligned} \mathrm{BR}_{H\to hh} &= \frac{\Gamma_{H\to hh}}{\Gamma_{\mathrm{tot}}}, \\ \mathrm{BR}_{H\to \mathrm{SM}} &= \sin^2\alpha \times \frac{\Gamma_{\mathrm{SM},H\to\mathrm{SM}}}{\Gamma_{\mathrm{tot}}}, \end{aligned} \tag{11}$$

where $\Gamma_{\mathrm{SM},\,H\to\mathrm{SM}}$ denotes the partial decay width of the SM Higgs boson and $H \to \mathrm{SM}$ represents any SM Higgs decay mode. The total width is given by

$$\Gamma_{\mathrm{tot}} \;=\; \sin^2\alpha \,\times\, \Gamma_{\mathrm{SM,\,tot}} + \Gamma_{H\to hh},$$

where $\Gamma_{\mathrm{SM,\,tot}}$ denotes the total width of the SM Higgs boson with mass m_H. The suppression by $\sin^2\alpha$ directly follows from the suppression of all SM–like couplings, cf. Eq. (6). For $\mu' = 0$, we recover the SM Higgs boson branching ratios.

For collider phenomenology, two features are important:

- the suppression of the *production cross section* of the two Higgs states induced by the mixing, which is given by $\sin^2\alpha\,(\cos^2\alpha)$ for the heavy (light) Higgs, respectively;
- the suppression of the *Higgs decay modes to SM particles*, which is realized if the competing decay mode $H \to hh$ is kinematically accessible.

For the high mass (low mass) scenario, i.e. the case where the light (heavy) Higgs boson is identified with the discovered Higgs state at ~ 125 GeV, $|\sin\alpha| = 0\,(1)$ corresponds to the complete decoupling of the second Higgs boson and therefore the SM-like scenario.

B. Model parameters

At the Lagrangian level, the model has five free parameters,

$$\lambda_1,\, \lambda_2,\, \lambda_3,\, v,\, x, \tag{12}$$

while the values of the additional parameters μ^2, m^2 are fixed by the minimization conditions.

A physical basis is given by

$$m_h,\, m_H,\, \alpha,\, v,\, \tan\beta \equiv \frac{v}{x}. \tag{13}$$

The vacuum expectation value of the Higgs doublet Φ is given by the SM value $v \sim 246$ GeV, and one of the Higgs masses is fixed to $m_{h/H} = 125.14\,\text{GeV}$. In this case, we are left with only three independent parameters,

$$m \equiv m_{H/h},\, \sin\alpha,\, \tan\beta$$

where the latter enters the collider phenomenology only via the additional decay channel $H \to hh$. Note that from a collider perspective, for cases where the decay mode $H \to h\,h$ is kinematically allowed, the *third* input variable could be replaced by either the total width the heavier state, the branching ratio BR $(H \to h\,h)$, or the partial decay width into this channel respectively, such that

$$\left\{m \equiv m_{H/h},\, \sin\alpha,\, \tan\beta\right\};\; \left\{m \equiv m_{H/h},\, \sin\alpha,\, \Gamma(H)\right\};\; \left\{m \equiv m_{H/h},\, \sin\alpha,\, \text{BR}(H \to h\,h)\right\}$$

are all viable parameter choices. If the insertion starts on the Lagrangian level (via e.g. FeynRules [7] or similar), also the Lagrangian parameters as such can be used as input values, but then care must be taken to correctly translate these into viable parameter regions.

II. CONSTRAINTS

Constraints have been extensively discussed in [1] and will therefore only shortly be repeated here.

A. Theory constraints

We consider

- vacuum stability and minimization of model up to a scale $\mu_{\text{run}} = 4 \times 10^{10}\,\text{GeV}$
- perturbative unitarity of the $2 \to 2$ 5-dimensional S-matrix, for (W^+W^-, ZZ, hh, hH, HH) initial/ final states respectively.
- perturbativity of the couplings in the potential, i.e. $|\lambda_i| \leq 4\pi$, up to a scale $\mu_{\text{run}} = 4 \times 10^{10}\,\text{GeV}$

B. Experimental constraints

The following experimental constraints have been taken into account at 95 % C.L.

- agreement mit electroweak precision observables comparing to oblique parameters S, T, U [8–11], and comparing to the values given in [12],
- agreement with the NLO calculation of the $W-$mass, as presented in [3], in comparison with the experimental value [13–15],
- agreement with limits from direct searches at LEP, Tevatron, and the LHC using `HiggsBounds` [16–19],
- agreement with Higgs signal strength for the 125 GeV Higgs, using `HiggsSignals` [20].

Note that for the latter two points results as available within the respective codes have been applied.

C. Summary of constraints

1. High mass region

The importance of the different constraints on the mixing angle $\sin\alpha$ in the high mass region, where $m_h \sim 125\,\mathrm{GeV}$, is best summarized in Figure 3 from [1], which we here show in Figure 1. Note that this angle regulates the *global* suppression of the production cross section with respect to production of Higgs bosons in the SM of the same mass. We see that the important constraints stem from direct searches ($m_H \lesssim 300\,\mathrm{GeV}$), the NLO corrections to the W-boson mass ($M_H \in [300\,\mathrm{GeV};\ 800\,\mathrm{GeV}]$), and perturbativity of the couplings ($m_H \geq 800\,\mathrm{GeV}$). Unfortunately, this leads to a relatively large suppression for the direct production of these particles, at LHC run II. Figure 2 shows the predicted production cross section at 14 TeV after all constraints have been taken into account. Note that these plots were obtained using a *simple rescaling* of production cross section of a SM Higgs Boson of the same mass as given in [21].

2. Low mass region

In the low mass region, where $m_H \sim 125\,\mathrm{GeV}$, the parameter space is extremely constrained from especially the agreement with the Higgs signal strength measurement and LEP constraints. Table III from [1] (Table I) summarizes these constraints. Note that here the SM decoupling corresponds to $|\sin\alpha| = 1$. Table V in the same reference (Table II here) gives direct production cross sections for the additional lighter states at a 8 and 14 TeV LHC, respectively. For the values presented there, similar constraints as discussed above apply.

III. BENCHMARKS FOR LHC RUN II

The benchmark points/ planes presented below have been chosen to give the *maximally* allowed production cross sections at a 14 TeV LHC.

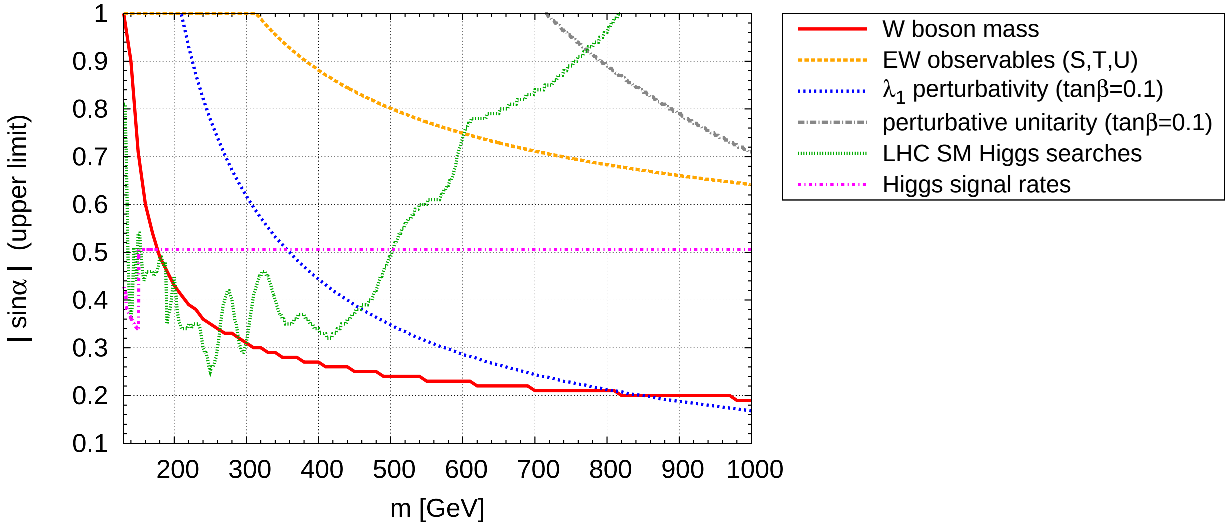

FIG. 1: Maximal allowed values for $|\sin\alpha|$ in the high mass region, $m_H \in [130, 1000]$ GeV, from NLO calculations of the W boson mass (*red, solid*) [3], electroweak precision observables (EWPOs) tested via the oblique parameters S, T and U (*orange, dashed*), as well as from the perturbativity requirement of the RG-evolved coupling λ_1 (*blue, dotted*), evaluated at $\tan\beta = 0.1$. For Higgs masses $m_H \lesssim 800$ GeV the NLO corrections to the W boson mass yield the strongest constraint.

A. Heavy scenario, $m_h \sim 125\,\mathrm{GeV}$, $|\sin\alpha|_{\mathbf{SM}} = 0$

We distinguish between two different search channels

- SM-like final states. For the heavy mass regime, the dominant SM branching ratio is the WW decay, as for Higgs bosons within the SM of the same mass. Therefore, maximizing the production cross section corresponds to maximizing the parameter

$$\kappa \equiv \frac{\sigma}{\sigma_{\mathrm{SM}}} \times \mathrm{BR}(H \to \mathrm{SM}) = \sin^4\alpha\,\frac{\Gamma_{\mathrm{SM,tot}}}{\Gamma_{\mathrm{tot}}},$$

- $h\,h$ final states. Here, the opposite applies, and the parameter

$$\kappa' \equiv \frac{\sigma}{\sigma_{\mathrm{SM}}} \times \mathrm{BR}(H \to hh) = \sin^2\alpha\,\frac{\Gamma_{H\to hh}}{\Gamma_{\mathrm{tot}}},$$

  needs to be maximized.

Results for the allowed ranges for these parameters can be found in Figure 3. The easiest way to quantify good benchmarks in this regime is to consider the *maximally* allowed mixing angle, together with the *maximal* and *minimal* branching ratio into hh. This then corresponds to benchmarks with a certain mass and a range for the additional branching ratio.

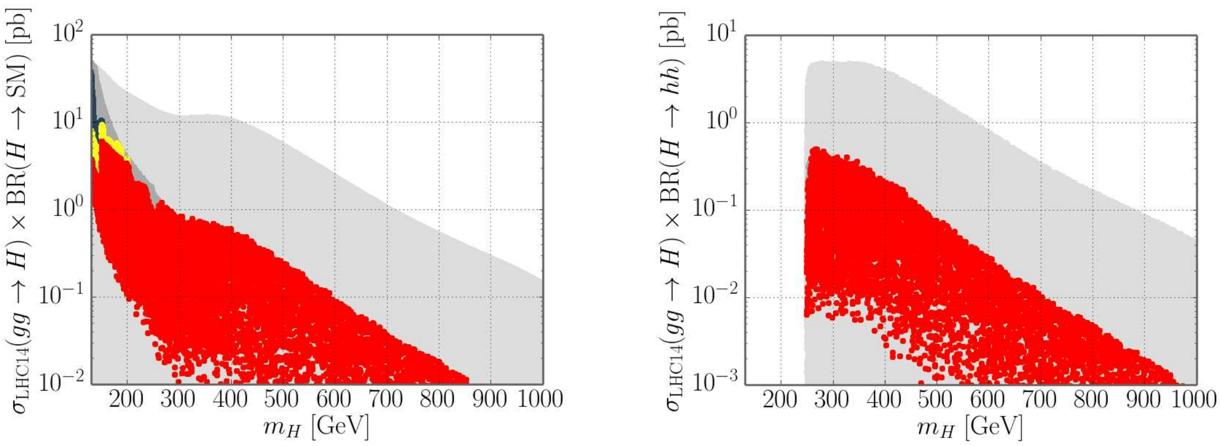

(a) Heavy Higgs signal rate with SM particles in the final state for the LHC at 14 TeV.

(b) Heavy Higgs signal rate with light Higgs bosons in the final state for the LHC at 14 TeV.

FIG. 2: LHC signal rates of the heavy Higgs boson H decaying into SM particles (a) or into two light Higgs bosons, $H \to hh$, (b), in dependence of the heavy Higgs mass, m_H, for CM energy of 14 TeV.

m_h [GeV]	$\lvert\sin\alpha\rvert_{\text{min, HB}}$	$\lvert\sin\alpha\rvert_{\text{min, HS}}$	$(\tan\beta)_{\text{max}}$	$(\tan\beta)_{\text{no } H\to hh}$
120	0.410	0.918	8.4	–
110	0.819	0.932	9.3	–
100	0.852	0.891	10.1	–
90	0.901	–	11.2	–
80	0.974	–	12.6	–
70	0.985	–	14.4	–
60	0.978	0.996	16.8	0.21
50	0.981	0.998	20.2	0.20
40	0.984	0.998	25.2	0.18
30	0.988	0.998	33.6	0.16
20	0.993	0.998	50.4	0.12
10	0.997	0.998	100.8	0.08

TABLE I: Table III from [1]. Limits on $\sin\alpha$ and $\tan\beta$ in the low mass scenario for various light Higgs masses m_h. The limits on $\sin\alpha$ have been determined at $\tan\beta = 1$. The lower limit on $\sin\alpha$ stemming from exclusion limits from LEP or LHC Higgs searches evaluated with `HiggsBounds` is given in the second column. If the lower limit on $\sin\alpha$ obtained from the test against the Higgs signal rates using `HiggsSignals` results in stricter limits, we display them in the third column. The upper limit on $\tan\beta$ in the fourth column stems from perturbative unitarity for the complete decoupling case ($|\sin\alpha| = 1$). In the fifth column we give the $\tan\beta$ value for which $\Gamma_{H\to hh} = 0$ is obtained, given the maximal mixing angle allowed by the Higgs exclusion limits (second column). At this $\tan\beta$ value, the $|\sin\alpha|$ limit obtained from the Higgs signal rates (third column) is abrogated.

m_h [GeV]	$\sigma_{gg}^{8\,\mathrm{TeV}}$[pb]	$\sigma_{gg}^{14\,\mathrm{TeV}}$[pb]
120	3.28	8.40
110	3.24	8.12
100	6.12	14.96
90	6.82	16.26
80	2.33	5.41
70	2.97	6.73
60	0.63	1.38
50	0.45	0.96
40	0.74	1.50

TABLE II: Table V from [1]. Maximally allowed cross sections, $\sigma_{gg} = \left(\cos^2\alpha\right)_{\mathrm{max}} \times \sigma_{gg,\mathrm{SM}}$, for direct light Higgs production at the LHC at CM energies of 8 and 14 TeV after all current constraints have been taken into account. The SM Higgs production cross sections have been taken from Ref. [21, 22].

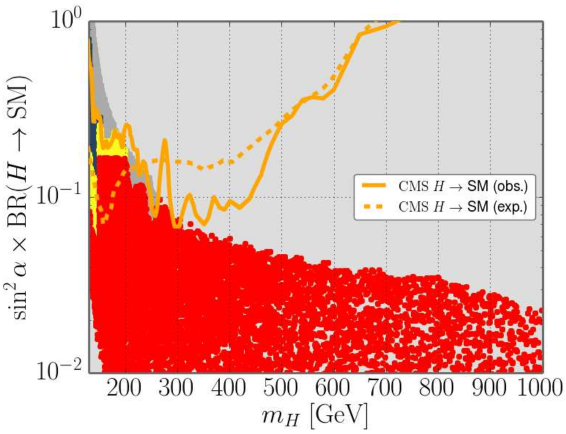

(a) Heavy Higgs signal rate with SM particles in the final state. The orange solid (dashed) curves indicate the observed (expected) 95% C.L. limits from the latest CMS combination of SM Higgs searches [23].

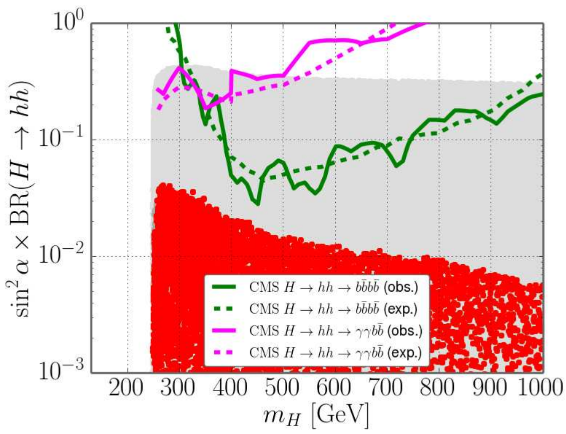

(b) Heavy Higgs signal rate with light Higgs bosons in the final state. We display the current expected and observed 95% C.L. limits from CMS $H \to hh$ searches with $\gamma\gamma b\bar{b}$ [24] and $b\bar{b}b\bar{b}$ [25] final states.

FIG. 3: Collider signal rates of the heavy Higgs boson H decaying into SM particles (a) or into two light Higgs bosons, $H \to hh$, (b), in dependence of the heavy Higgs mass, m_H. The rates are normalized to the inclusive SM Higgs production cross section at the corresponding mass value [21, 26, 27].

We need to distinguish scenarios for which the additional decay mode is allowed/ forbidden[1]. For the latter, the additional parameter is $\tan\beta$, which should be kept in allowed regimes for consistency reasons. Benchmark stripes for both cases are given in Tables III and IV, respectively[2].

[1] This refers to onshell approximations.
[2] Note that these benchmarks also obey the limits in [28], which have appeared after the study in [1].

m_H[GeV]	$|\sin\alpha|_{\text{max}}$	$\tan\beta_{\text{max}}$
130	0.42	1.79
135	0.38	1.73
140	0.36	1.67
145	0.35	1.62
150	0.34	1.57
[155; 170]	0.51	[1.44; 1.56]
175	0.46	1.40
180	0.44	1.37
185	0.45	1.33
190	0.44	1.27
195	0.45	1.25
200	0.43	1.23
205	0.42	1.18
210	0.41	1.15
215	0.4	1.12
220	0.39	1.10
[225; 230]	0.38	1.07
235	0.37	1.03
[240; 245]	0.36	[0.97; 1.00]

TABLE III: Benchmark points for mass ranges where the onshell decay $H \to h\,h$ is kinematically forbidden. Maximal values of $\tan\beta$ were calculated at the maximal mixing angle, and should be applied for consistency reasons.

Results for intermediate masses not tabulated should as a first approximation be interpolated.

B. Light scenario, $m_H \sim 125\,\text{GeV},\ |\sin\alpha|_{\mathbf{SM}} = 1$

As discussed above, for the case that

$$m_H \sim 125\,\text{GeV},$$

$|\sin\alpha| = 1$ corresponds to the SM limit, and deviations from this value parametrize the new physics contributions. As before, in principle two different channels are interesting

- *direct production* of the lighter state m_h,
- measurement through the *decays* $H(125\,\text{GeV}) \to h\,h$.

For direct production, small $|\sin\alpha|$ values are of interest, and minimally allowed values for $|\sin\alpha|$ are given in Table I; Table II list the respective direct production cross sections. For the option that the additional decay channel is open, we list maximal branching ratios for the decay $H \to h\,h$ in Table V. The lighter Higgses then decay further according to the branching ratios of a SM Higgs of the respective mass.

m_H[GeV]	$\lvert\sin\alpha\rvert_{\max}$	$BR^{H\to hh}_{\min}$	$BR^{H\to hh}_{\max}$
$[250;255]$	0.35	$[0.12;0.17]$	0.26;
$[260;265]$	0.34	0.18	$[0.33;0.36]$
270	0.31	0.18	0.38
275	0.28	0.18	0.39
280	0.29	0.18	0.39
$[285;290]$	0.32	$[0.20;0.26]$	$[0.40;0.41]$
$[295;305]$	0.31	$[0.23;0.27]$	$[0.40;0.41]$
310	0.28	0.21	0.39
$[315;325]$	0.26	$[0.11;0.14]$	0.39
330	0.28	0.11	0.38
$[335;345]$	0.29	$[0.17;0.22]$	0.38
$[350;360]$	0.28	$[0.21;0.23]$	$[0.36;0.37]$
$[365;405]$	0.27	$[0.18;0.20]$	$[0.31;0.35]$
$[410;440]$	0.26	$[0.16;0.21]$	$[0.27;0.30]$
$[445;485]$	0.25	$[0.14;0.18]$	$[0.23;0.25]$
$[490;540]$	0.24	$[0.16;0.18]$	$[0.22;0.25]$
$[545;610]$	0.23	$[0.17;0.19]$	$[0.22;0.24]$
$[615;695]$	0.22	$[0.18;0.19]$	$[0.22;0.24]$
$[700;825]$	0.21	0.19	$[0.22;0.23]$
$[830;865]$	0.20	0.19	0.22
$[870;905]$	0.19	0.19	$[0.21;0.22]$
$[910;955]$	0.18	0.19	$[0.21;0.22]$
$[960;1000]$	0.17	0.19	0.21

TABLE IV: Maximal and minimal allowed branching ratios, taken at the maximal allowed value of $\lvert\sin\alpha\rvert$. Note that miminal values for the BR stem from $\sin\alpha\,\leq\,0$.

m_h[GeV]	$\sin\alpha$	$BR^{H\to hh}_{\max}$
60	0.9996	0.225
50	0.9998	0.251
40	0.9996	0.255
30	0.9999	0.253
20	0.9999	0.251
10	0.9996	0.248

TABLE V: Maximal branching ratios for $H\,\to\,h\,h$. This BR can always be zero for the choice $\tan\beta\,=\,-\arctan\,\alpha$. Results have been obtained using a linear grid.

C. Comments regarding tools

All cross-section predictions presented here are based on simple *rescaling* of SM production cross sections taken from [21], and especially lack contributions due to interference with the additional scalar. Tools which can handle these have been presented e.g. in [29–32]; therefore, experimental cross sections should be calculated using the above tools.

IV. CONCLUSIONS

We have presented benchmark ranges for a model where the Higgs sector is extended by an additional scalar which transforms trivially under the SM gauge groups. We have presented values for all possible channels, i.e. where the second Higgs decays into SM-like particles, or where the heavier Higgs decays into two lighter ones. These benchmarks include all current bounds in this model, and are designed to maximize the respective cross-sections at LHC run II.

---

[1] T. Robens and T. Stefaniak, Eur. Phys. J. **C75**, 104 (2015), 1501.02234.
[2] G. M. Pruna and T. Robens, Phys.Rev. **D88**, 115012 (2013), 1303.1150.
[3] D. Lopez-Val and T. Robens, Phys.Rev. **D90**, 114018 (2014), 1406.1043.
[4] R. Schabinger and J. D. Wells, Phys.Rev. **D72**, 093007 (2005), hep-ph/0509209.
[5] B. Patt and F. Wilczek (2006), hep-ph/0605188.
[6] M. Bowen, Y. Cui, and J. D. Wells, JHEP **0703**, 036 (2007), hep-ph/0701035.
[7] N. D. Christensen and C. Duhr, Comput. Phys. Commun. **180**, 1614 (2009), 0806.4194.
[8] G. Altarelli and R. Barbieri, Phys. Lett. B **253**, 161 (1991).
[9] M. E. Peskin and T. Takeuchi, Phys.Rev.Lett. **65**, 964 (1990).
[10] M. E. Peskin and T. Takeuchi, Phys.Rev. **D46**, 381 (1992).
[11] I. Maksymyk, C. Burgess, and D. London, Phys.Rev. **D50**, 529 (1994), hep-ph/9306267.
[12] M. Baak et al. (Gfitter Group), Eur.Phys.J. **C74**, 3046 (2014), 1407.3792.
[13] J. Alcaraz et al. (ALEPH Collaboration, DELPHI Collaboration, L3 Collaboration, OPAL Collaboration, LEP Electroweak Working Group) (2006), hep-ex/0612034.
[14] T. Aaltonen et al. (CDF Collaboration), Phys.Rev.Lett. **108**, 151803 (2012), 1203.0275.
[15] V. M. Abazov et al. (D0 Collaboration), Phys.Rev. **D89**, 012005 (2014), 1310.8628.
[16] P. Bechtle, O. Brein, S. Heinemeyer, G. Weiglein, and K. E. Williams, Comput. Phys. Commun. **181**, 138 (2010), 0811.4169.
[17] P. Bechtle, O. Brein, S. Heinemeyer, G. Weiglein, and K. E. Williams, Comput. Phys. Commun. **182**, 2605 (2011), 1102.1898.
[18] P. Bechtle, O. Brein, S. Heinemeyer, O. Stål, T. Stefaniak, et al., PoS **CHARGED2012**, 024 (2012), 1301.2345.
[19] P. Bechtle, O. Brein, S. Heinemeyer, O. Stål, T. Stefaniak, et al., Eur. Phys. J. C **74**, 2693 (2013), 1311.0055.
[20] P. Bechtle, S. Heinemeyer, O. Stål, T. Stefaniak, and G. Weiglein, Eur.Phys.J. **C74**, 2711 (2014), 1305.1933.
[21] S. Heinemeyer et al. (The LHC Higgs Cross Section Working Group) (2013), 1307.1347.
[22] M. Grazzini. Private communication.
[23] CMS Collaboration (2012), cMS-PAS-HIG-12-045.
[24] CMS Collaboration (CMS Collaboration) (2014), cMS-PAS-HIG-13-032.
[25] CMS Collaboration (CMS Collaboration) (2014), cMS-PAS-HIG-14-013.

[26] S. Dittmaier et al. (LHC Higgs Cross Section Working Group) (2011), 1101.0593.
[27] S. Dittmaier, S. Dittmaier, C. Mariotti, G. Passarino, R. Tanaka, et al. (2012), 1201.3084.
[28] V. Khachatryan et al. (CMS) (2015), 1504.00936.
[29] E. Maina, JHEP **06**, 004 (2015), 1501.02139.
[30] N. Kauer and C. O'Brien, Eur. Phys. J. **C75**, 374 (2015), 1502.04113.
[31] A. Ballestrero and E. Maina (2015), 1506.02257.
[32] S. Dawson and I. M. Lewis (2015), 1508.05397.